PHYSICAL REVIEW A VOLUME 35, NUMBER 1 JANUARY 1, 1987

Theory of the Rydberg-atom two-photon micromaser

M. Brune, J. M. Raimond, and S. Haroche
Laboratoire de Spectroscopie Hertzienne de l'Ecole Normale Supérieure, 24 rue Lhomond, 75231 Paris Cédex 05, France
(Received 31 July 1986)

A continuous-wave maser operating on a two-photon transition between Rydberg levels is expected to oscillate with about one atom and a few tens of microwave photons at any time in its superconducting cavity. We analyze in detail the characteristics of this new microscopic quantum electronics device presently under construction in our laboratory.

I. INTRODUCTION

Lasers operating on two-photon atomic transitions have been widely studied in theoretical papers over the last twenty years.[1–11] The continuous operation of such systems would present many interesting features, making it very different from ordinary one-photon lasers (field dynamics and photon statistics in particular are quite different in one- and two-photon oscillators[9,11]). To our knowledge however, only one report of two-photon amplification in a pulsed system[12] has been published up to now and, in spite of numerous attempts, no realization so far of a cw two-photon oscillator has been successful. This is due to severe experimental difficulties related to extremely low two-photon gain in usual transitions and to the existence of very strong competing nonlinear processes[6] (multiple-wave mixing and stimulated Raman effect tend to deplete the pumped level before two-photon amplification can take place). In this paper we show that Rydberg atoms in a superconducting cavity seem to provide an answer to the various problems mentioned above and we describe the principle of an experiment in progress in our laboratory to realize a cw two-photon maser.

Rydberg-atoms—cavity systems have in the past years developed into new kinds of quantum electronic devices, with fascinating characteristics; Rydberg masers with very low thresholds,[13] down to a single atom at a time in the cavity either in a transient[14] or in the cw (Ref. 15) regime have been obtained and the theory of these "micromasers" has been derived in detail.[13,16–19]

The advantages of Rydberg atoms for these studies lie in their very large electric dipole coupling to radiation and to their long-wavelength resonances, making it possible to realize low-order closed very-high-Q cavities. The combination of these factors explains the reduction of the threshold down to a single atom in these systems. These oscillators have been restricted so far to one-photon-allowed transitions ($nS \rightarrow n'P$ or $nP \rightarrow n'D$ transitions in Na, Cs, and Rb atoms; n and n' are the principal quantum numbers and S, P, and D refer, respectively, to 0,1,2 angular momentum states).

For two-photon transitions, Rydberg atoms offer another very attractive feature: a relay level can be found in the Rydberg-states spectrum nearly halfway between the initial and the final levels of the transition, thus greatly enhancing the two-photon transition amplitude.[20–22] Figure 1 shows the relevant levels in an alkali-metal Rydberg-state energy diagram. The transition of interest occurs between the nS and $(n-1)S$ states and is thus two-photon allowed and one-photon forbidden. To simplify the notations, these states will be called $|e\rangle$ and $|f\rangle$ in the following (energies E_e and E_f). The intermediate level $(n-1)P_{3/2}$ (called $|i\rangle$, energy E_i) is detuned by the amount

$$\hbar\Delta = E_i - \frac{(E_e + E_f)}{2} \tag{1}$$

from the average of the energies of the $|e\rangle$ and $|f\rangle$ states.[23]

The quantum defects of the nS and $nP_{1/2,3/2}$ series differing in all alkali metals by about 0.5, $\hbar\Delta$ turns out to be quite generally a small fraction of the energy interval $E_e - E_f$. Moreover, there is a slow variation with n of the quantum defects, which has been measured in detail in very precise spectroscopic experiments.[24–27] This variation entails that Δ crosses zero value around experimentally accessible n values in rubidium and cesium; we show in Fig. 2 the detuning of the $(n-1)P_{3/2}$ level as a function of the principal quantum number $(n-1)$ for these two species. It appears that Δ is exceedingly small for $n-1=39$ in rubidium and $n-1=43$ in cesium ($\Delta/2\pi = -39$ MHz and -33.3 MHz, respectively). The corresponding $nS \rightarrow (n-1)S$ transitions are particularly

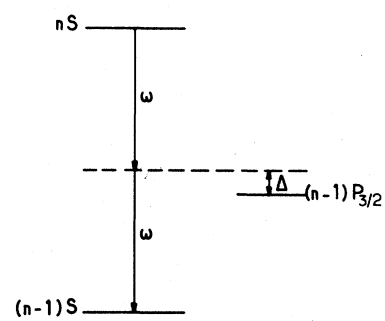

FIG. 1. Energy levels relevant to the two-photon Rydberg maser.

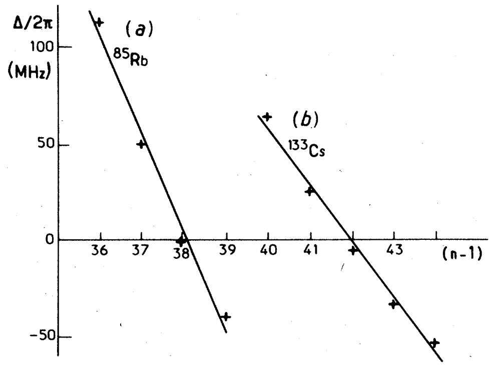

FIG. 2. Variation with the principal quantum number n of the detuning $\Delta/2\pi$ of the $(n-1)P_{3/2}$ state from $(E_e+E_f)/2h$. (a) for ^{85}Rb. (b) for ^{133}Cs. Data are deduced from Refs. 26 and 25, respectively.

well suited for two-photon amplification. [The detuning is even smaller for $n-1=38$ in Rb and $n-1=42$ in Cs. It is then, however, so small that is is difficult to discriminate the direct two-photon $nS \rightarrow (n-1)S$ process from the resonant one-photon cascade $nS \rightarrow (n-1)P_{3/2} \rightarrow (n-1)S$. We thus choose in the following to consider the very small but nonzero detunings corresponding to $n-1=39$ in Rb or 43 in Cs; see Sec. V.]

We show in this paper that a two-photon maser operating on a degenerate two-photon transition between these levels in a $Q \sim 10^8$ cavity should oscillate with only about one atom at a time in the cavity and a few tens of microwave photons. Such a micromaser is in principle quite similar to the one-photon masers already operating in Rydberg transitions.[15,19] Due to the extremely low field intensities in the cavity, the potentially damaging nonlinear competing effects mentioned above should in this case remain negligible, as well as the cavity nonresonant one-photon amplification towards the intermediate level $|i\rangle$.

The outline of this paper is as follows. In Sec. II we present a qualitative semiclassical analysis of the two-photon maser operation and give an estimate of the threshold and field intensity in the cavity. This intensity being very small, a full quantum description of the basic interaction process between the atoms and radiation, including spontaneous as well as stimulated effects, appears necessary. We present this analysis in Sec. III where we use the dressed-atom formalism to describe the two-photon Rabi nutation of a Rydberg atom in a quantized field. We are then able, in Sec. IV, to present a more quantitative but nevertheless simple model of the two-photon Rydberg maser and we calculate some important characteristics such as the average field evolution and the photon-number variance under various conditions. Conclusions of this study are presented in Sec. V.

II. QUALITATIVE ANALYSIS OF THE TWO-PHOTON RYDBERG MICROMASER

Assume that atoms with the level configuration of Fig. 1 cross a cavity tuned to the frequency

$$\omega = \frac{(E_e - E_f)}{2\hbar} . \tag{2}$$

This cavity contains a field which—in the present qualitative analysis—is supposed to correspond to a large average photon number $\bar{N}$ ($\bar{N} \gg 1$), so that the atom-field interaction can be considered as purely classical.

The atoms are initially prepared in the excited state $|e\rangle$ and they undergo in the cavity a coherent second-order Rabi nutation process between the levels $|e\rangle$ and $|f\rangle$. The order of magnitude of this nutation frequency can be evaluated in a very simple way. The field amplitude associated with $\bar{N}$ photons in a cavity of frequency ω and volume V is

$$\mathscr{E}(\bar{N}) \simeq \mathscr{E}_0 \sqrt{\bar{N}} \tag{3}$$

with

$$\mathscr{E}_0 = \left[\frac{\hbar\omega}{2\epsilon_0 V} \right]^{1/2} \tag{4}$$

being the field "per photon" in this cavity. The couplings of the allowed atomic transition $|e\rangle \rightarrow |i\rangle$ and $|i\rangle \rightarrow |f\rangle$ to the field in this cavity are defined by the elementary one-photon Rabi frequencies

$$\Omega_{ei} = -\frac{\langle e | D | i \rangle \mathscr{E}_0}{\hbar} \tag{5a}$$

and

$$\Omega_{if} = -\frac{\langle i | D | f \rangle \mathscr{E}_0}{\hbar} , \tag{5b}$$

where $\langle e | D | i \rangle$ and $\langle i | D | f \rangle$ are the matrix elements of the electric dipole operator D (assumed to be real).

If the cavity were tuned in resonance with the first-order one-photon transitions $|e\rangle \rightarrow |i\rangle$ or $|i\rangle \rightarrow |f\rangle$, the atom would undergo an ordinary one-photon Rabi precession between the corresponding levels at frequencies proportional to the field amplitude $\mathscr{E}_0\sqrt{\bar{N}}$, i.e., very close to $\Omega_{ei}\sqrt{\bar{N}}$ and $\Omega_{if}\sqrt{\bar{N}}$, respectively (we neglect here the change of $\mathscr{E}_0$ when ω and V are slightly modified to put the field in resonance with the one-photon transitions).

When the cavity is in resonance with the two-photon $|e\rangle \rightarrow |f\rangle$ transition instead, the Rabi precession occurs between levels coupled to second order by a matrix element given in frequency units as

$$\Omega_{ef}(\bar{N}) \simeq \frac{\Omega_{ei}\sqrt{\bar{N}}\,\Omega_{if}\sqrt{\bar{N}}}{\Delta} = \frac{\Omega_{ei}\Omega_{if}\bar{N}}{\Delta} . \tag{6}$$

More precisely, the probability $P_e(t)$ to find at time t the atom in level $|e\rangle$, if it has been prepared in this level at time zero, is given by the well-known Rabi formula generalized to two-photon processes[21]

$$P_e(t) \simeq 1 - \sin^2[\Omega_{ef}(\bar{N})t] = \tfrac{1}{2}\{1 + \cos[\Omega(\bar{N})t]\} \tag{7}$$

with the Rabi precession frequency given by

$$\Omega(\bar{N}) = 2\Omega_{ef}(\bar{N}) = \frac{2\Omega_{ei}\Omega_{if}\bar{N}}{\Delta} . \tag{8}$$

We get a pulsation proportional to $\bar{N}$, i.e., to the field intensity (and not to the field amplitude as in the case for ordinary one-photon transitions) and inversely proportional to the frequency mismatch Δ, which corresponds to the enhancement effect discussed in Sec. I.

Let us notice at this stage that the above results—obtained by qualitative and semi-intuitive arguments—are at best approximate. The field, described only by an average photon number, is considered here as "classical" and spontaneous emission in the cavity mode is neglected. Moreover, we have only considered the second-order coupling between $|e\rangle$ and $|f\rangle$ and disregarded the dynamical Stark shifts[20,22] induced by the field slightly off-resonant with the $|e\rangle \rightarrow |i\rangle$ and $|i\rangle \rightarrow |f\rangle$ transitions. These shifts are also second-order effects in the atom-field coupling and inversely proportional to Δ. Δ is so small here that these effects cannot *a priori* be neglected even for relatively small fields. If the cavity is resonant with the free two-photon atomic transition frequency [Eq. (2)], it is no longer exactly resonant for the shifted level transition and the Rabi frequency must accordingly be modified. All these effects will be considered in Sec. III and we will show then that Eqs. (7) and (8) describe qualitatively correctly the Rabi precession between levels $|e\rangle$ and $|f\rangle$, provided the average number of photons is large compared to unity and Ω_{ei} is not too different from Ω_{if}.

Another approximation comes, of course, from the fact that we consider here only one relay level and neglect all the other states of the atom not represented on Fig. 1. This is, however, a very good approximation since Δ is very small compared to all the other frequency mismatches.

Due to the large value of $\langle e|D|i\rangle$ and $\langle i|D|f\rangle$ (proportional to n^2 in Rydberg levels), the frequencies Ω_{ei} and Ω_{if} are intrinsically huge. Let us consider here the case of the $40S \rightarrow 39P$ and $39P \rightarrow 39S$ transitions in rubidium at $\omega/2\pi = 68.415$ GHz, in a cavity of volume $V \simeq 70$ mm^3. We find then with the matrix elements $\langle e|D|i\rangle = 1443qa_0$ and $\langle i|D|f\rangle = 1479qa_0$,

$$\Omega_{ei} \sim \Omega_{if} \sim 7\times10^5\ \mathrm{s}^{-1} .$$

Combining these values with $\Delta/2\pi = -39$ MHz, we get from Eq. (8),

$$\Omega(\overline{N}) \simeq -B\overline{N} \tag{9}$$

with $B = 4000\ \mathrm{s}^{-1}$. The two-photon Rabi pulsation is thus as large as $10^5\ \mathrm{s}^{-1}$ for a field of only about 25 photons.

With this order of magnitude in mind, the principle of a Rydberg two-photon micromaser appears very simple: Rydberg atoms are prepared by laser irradiation in the upper level $|e\rangle = |nS\rangle$ and cross a microwave cavity having a damping time $t_{\mathrm{cav}} = Q/\omega$ (Q is the cavity-quality factor). The time separating consecutive atoms in the cavity is t_{at}, each atom interacting with the field during its transit time t_{int}. The condition

$$t_{\mathrm{at}} \geq t_{\mathrm{int}} \tag{10}$$

ensures that the number of atoms at any time in the cavity is of the order of one (micromaser condition), whereas the condition

$$t_{\mathrm{cav}} \gg t_{\mathrm{at}}, t_{\mathrm{int}} \tag{11}$$

means that a large absolute number of photons will eventually be able to build up.

We have symbolized this system in Fig. 3 where we have assumed for sake of simplicity a regular flow of atoms, separated by a distance L, crossing the cavity of length l at a constant velocity v. Then one obviously has $t_{\mathrm{int}} = l/v$ and $t_{\mathrm{at}} = L/v$ with the condition $L \geq l$.

A qualitative estimate of the operating parameters of such a device is given by the following equations:

$$\Omega(\overline{N}) t_{\mathrm{int}} \sim r , \tag{12}$$

which implies that each atom yields a large fraction (ideally all) of its energy to the field, and

$$\overline{N} = \frac{2t_{\mathrm{cav}}}{t_{\mathrm{at}}} , \tag{13}$$

which means that the atomic flux is able to maintain the $\overline{N}$-photon field in the cavity [each atom leaves two photons, hence the factor 2 in Eq. (13)].

Combining Eqs. (12) and (13) with Eq. (9), we get

$$\frac{1}{t_{\mathrm{at}}} = \frac{\pi}{2Bt_{\mathrm{int}}t_{\mathrm{cav}}} . \tag{14}$$

With a quality factor $Q = 2\times10^8$—feasible with a niobium superconducting cavity at this frequency[26,28]—we have $t_{\mathrm{cav}} = Q/\omega \simeq 4.7\times10^{-4}$ s. On the other hand, $t_{\mathrm{int}} \sim 2.5\times10^{-5}$ s for a 7.5-mm-long cavity crossed at thermal velocity ($v = 300$ m/s). Taking the B value quoted above, we then get

$$\frac{1}{t_{\mathrm{at}}} = 3.3\times10^4\ \mathrm{s}^{-1} \tag{15}$$

and

$$\overline{N} = \frac{2t_{\mathrm{cav}}}{t_{\mathrm{at}}} \simeq 30 . \tag{16}$$

The atomic flux given by Eq. (15) should be easy to achieve with cw laser excitation of an atomic beam.[29] The corresponding value $t_{\mathrm{at}} = 3\times10^{-5}$ s is consistent with condition (10).

For a slightly more quantitative analysis of the system operation, we can write the rate equation giving the photon number evolution in the cavity,

$$\frac{d\overline{N}}{dt} = -\frac{\overline{N}}{t_{\mathrm{cav}}} + \frac{2}{t_{\mathrm{at}}}\left[\frac{1-\cos[\Omega(\overline{N})t_{\mathrm{int}}]}{2}\right] . \tag{17}$$

The average photon number $\overline{N}$ evolves under the com-

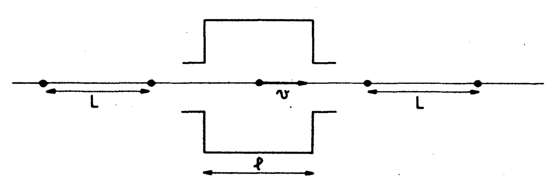

FIG. 3. Scheme of the two-photon micromaser.

bined effects of the cavity losses [first term in the right-hand side of Eq. (17)] and the atomic Rabi nutation process (second term); for each atom undergoing a pulse of "area" Ωt_{int}, a "fraction"

$$\frac{1-\cos[\Omega(\overline{N})t_{\text{int}}]}{2}$$

of the photon pair is released in the cavity and this process repeats itself at the rate t_{at}^{-1}.

Figure 4 represents the variations with $\overline{N}$ of the cavity-loss and atomic-gain terms, respectively, for increasing atomic fluxes. The losses are linear in $\overline{N}$ and the gain curve appears as a cosine function of $\overline{N}$. $\Omega(\overline{N})$ has been chosen so that a π pulse corresponds to $\overline{N}=30$. The t_{at} values of curves a, b, c, d correspond, respectively, to $t_{\text{at}}=0.17t_{\text{cav}}$, $t_{\text{at}}=8.4\times10^{-2}t_{\text{cav}}$, $t_{\text{at}}=4.2\times10^{-2}t_{\text{cav}}$, and $t_{\text{at}}=2.1\times10^{-2}t_{\text{cav}}$.

A possible operating point of the maser is represented by an intersection between the loss and gain curves. This point will be a stable solution if the gain slope is smaller than the loss one (stable solutions are shown by open circles on the figure). Threshold is reached for the gain curve b. It corresponds to $t_{\text{at}}=8.4\times10^{-2}t_{\text{cav}}$, i.e., $t_{\text{at}}=4\times10^{-5}$ s for $t_{\text{cav}}=4.7\times10^{-4}$ s, a value in good agreement with the above qualitative estimate. Curve a corresponds to a maser below threshold (no intersection other than $\overline{N}=0$ between loss and gain curves) whereas curves c and d correspond to an oscillating system.

Above threshold, the $\overline{N}=0$ point is classically stable (since the loss linear in $\overline{N}$ is larger than the gain quadratic in $\overline{N}$ around $\overline{N}=0$). In the semiclassical theory, the two-photon maser needs to be triggered by an initial field corresponding to an average photon number larger than the abscissa of the first nonzero crossing of the gain and loss curves (shown by black circles on curves c and d). The field will evolve according to Eq. (17) and eventually stabilize on a open circle solution. (A one-photon maser above threshold will, on the other hand, always start on "spontaneous" or "blackbody" noise without external triggering.) We will not discuss here in more detail this well-known feature of two-photon maser or laser devices.[5,7]

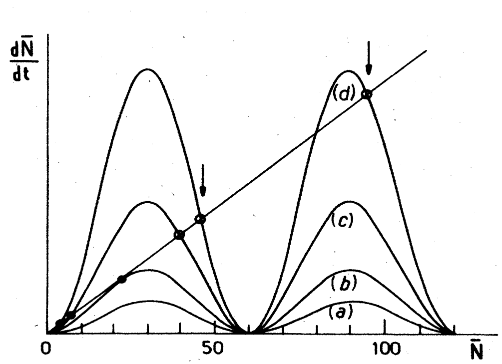

FIG. 4. Classical model of the two-photon maser: loss and gain contributions to $d\overline{N}/dt$ vs $\overline{N}$. The loss term is linear in $\overline{N}$ and the gain term a cosine function of $\overline{N}$. Curves a, b, c, and d correspond to the decreasing $t_{\text{at}}/t_{\text{cav}}$ values given in the text. Threshold corresponds to curve b. Stable operation points are shown by open circles.

Figure 4 also shows the possibility of multistable operation[5] for high pumping rates (two stable intersections of the gain and loss curves shown by arrows on curve d). This multistable behavior depends, however, on the fact that there are no fluctuations of t_{at} and t_{int} in this simple model and disappear if the atoms are introduced with random rates and velocities in the cavity.

III. TWO-PHOTON RABI NUTATION: AN EXACT QUANTUM-MECHANICAL DESCRIPTION

It has been shown[20,22] that the coherent evolution of an atomic system in a field resonant with a two-photon transition can be described as the evolution of a two-level or pseudospin-$\frac{1}{2}$ system (represented by a Bloch vector) rotating in a fictitious static field whose amplitude is proportional to the two-photon Rabi frequency. This pseudospin model, however, is based on a classical description of the field and applies only to usual situations where there is a very large absolute photon number in the cavity. A full quantum-mechanical treatment of the two-photon Rabi precession has been recently derived by Yoo and Eberly.[30] This treatment, valid for arbitrarily small photon numbers, is well adapted to the two-photon micromaser case and takes into account all the effects neglected in the intuitive approach of Sec. II. In this section, we adapt this treatment to our problem and derive—with the notations introduced in Sec. II—the exact expression of the two-photon Rabi frequency and Rabi nutation signals—only approximated by Eqs. (8) and (7). These expressions include both spontaneous- and stimulated-emission processes and take into account the dynamical Stark shifts induced by the quantized field on the atomic system.

It is convenient here to make use of the dressed-atom formalism in which one considers the eigenvalues and eigenstates of the combined atom plus field Hamiltonian.[31] This Hamiltonian can be written as

$$H=H_{\text{at}}+H_F+H_{\text{int}} \tag{18}$$

with H_{at}, H_F, and H_{int} being, respectively, the atom, field, and interaction terms

$$H_{\text{at}}=E_e\,|e\rangle\langle e\,|+E_i\,|i\rangle\langle i\,|+E_f\,|f\rangle\langle f\,| , \tag{19}$$

$$H_F=\hbar\omega(a^\dagger a+\tfrac{1}{2}) , \tag{20}$$

$$H_{\text{int}}=\hbar\Omega_{ei}(a\,|e\rangle\langle i\,|+a^\dagger\,|i\rangle\langle e\,|) + \hbar\Omega_{if}(a\,|i\rangle\langle f\,|+a^\dagger|f\rangle\langle i\,|) . \tag{21}$$

In these equations, a and $a^\dagger$ are the photon annihilation and creation operators, Ω_{ei} and Ω_{if} are given by Eqs. (5a) and (5b). In H_{int}, we have made the rotating-wave approximation which amounts to neglecting terms such as $a^\dagger|e\rangle\langle i\,|$ which couple levels whose energies differ by $E_e-E_i+\hbar\omega\simeq2\hbar\omega$.

Figure 5(a) represents the energy levels of the Hamiltonian $H_{\text{at}}+H_F$, neglecting for the moment the atom-field coupling. The energy diagram consists of a succession of triplet manifolds $|e,N\rangle$, $|i,N+1\rangle$, $|f,N+2\rangle$ separated from each other by one-photon energy $\hbar\omega$. These levels represent the atomic states $|e\rangle$, $|i\rangle$, and $|f\rangle$ with N, $N+1$, and $N+2$ photons, respectively, in the cavity. We assume also for the sake of simplicity that the field is exactly resonant with the two-photon transition [Eq. (2)] so that in each manifold the levels $|e,N\rangle$ and $|f,N+2\rangle$ are strictly degenerate. This assumption is, of course, not essential and could be relaxed at the expense of a slight complication of the following equations. The level $|i,N+1\rangle$ is separated from the $|e,N\rangle, |f,N+2\rangle$ doublet by the mismatch $\hbar\Delta$, much smaller than $\hbar\omega$.

Let us now take H_{int} into account. There is no coupling at all between different N manifolds. Within the Nth manifold ($|e,N\rangle$, $|i,N+1\rangle$, $|f,N+2\rangle$ levels in this order), H_{int} is represented by the matrix

$$H_{\text{int}}^{(N)}=\hbar\begin{bmatrix}0 & \Omega_{ei}\sqrt{N+1} & 0\\ \Omega_{ei}\sqrt{N+1} & 0 & \Omega_{if}\sqrt{N+2}\\ 0 & \Omega_{if}\sqrt{N+2} & 0\end{bmatrix}. \quad (22)$$

Carrying out the exact diagonalization of H_{int}, we find the three dressed energies [measured from the energy $E_e+(N+\frac{1}{2})\hbar\omega$ of state $|eN\rangle$],

$$E_{\pm}(N)=\frac{\hbar\Delta}{2}[1\pm\sqrt{1+(4/\Delta)\Omega(N)}]\ ,$$
$$E_0(N)=0\ , \quad (23)$$

corresponding to the normalized eigenstates

$$|\pm,N\rangle=\frac{\Omega_{ei}\sqrt{N+1}}{\frac{\Delta}{2}\left[1\pm\left[1+\frac{4\Omega(N)}{\Delta}\right]^{1/2}\right]}\frac{1}{K_{\pm}}|e,N\rangle+\frac{1}{K_{\pm}}|i,N+1\rangle+\frac{\Omega_{if}\sqrt{N+2}}{\frac{\Delta}{2}\left[1\pm\left[1+\frac{4\Omega(N)}{\Delta}\right]^{1/2}\right]}\frac{1}{K_{\pm}}|f,N+2\rangle\ ,$$
$$|0,N\rangle=\frac{\Omega_{if}\sqrt{N+2}}{\sqrt{\Delta\Omega(N)}}|e,N\rangle-\frac{\Omega_{ei}\sqrt{N+1}}{\sqrt{\Delta\Omega(N)}}|f,N+2\rangle\ . \quad (24)$$

In these equations, we define the frequency

$$\Omega(N)=\frac{\Omega_{ei}^2(N+1)+\Omega_{if}^2(N+2)}{\Delta} \quad (25)$$

and the normalization constant

$$K_{\pm}=\left[1+\frac{1}{1+\frac{\Delta}{2\Omega(N)}\left[1\pm\left[1+\frac{4\Omega(N)}{\Delta}\right]^{1/2}\right]}\right]^{1/2}. \quad (26)$$

In the situation of interest here, we can approximate these formulas by much simpler and nevertheless quite accurate ones by remarking that $\Omega(N)/\Delta$ is very small.

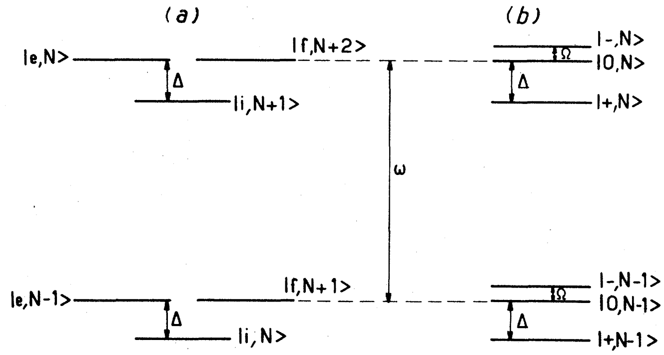

FIG. 5. Energy diagram of the atom-field system. (a) Coupling neglected. (b) Coupling taken into account: dressed states.

With $\Omega_{ei}\sim\Omega_{if}\sim 7\times10^5\ \text{s}^{-1}$ and $\Delta/2\pi=-39$ MHz, we have indeed

$$\Omega(0)=\frac{\Omega_{ei}^2+2\Omega_{if}^2}{\Delta}\simeq-6\times10^3\ \text{s}^{-1}$$

and $|\Omega(0)/\Delta|\simeq10^{-5}$. Even with N as large as 10^3, we still have $|\Omega(N)/\Delta|\leq10^{-2}$. It is thus legitimate to expand the exact solution in powers of Ω/Δ and to retain the first-order term. We then get

$$E_+(N)\simeq\hbar\Delta\ ,$$
$$E_-(N)=-\hbar\Omega(N)\ , \quad (27)$$
$$E_0(N)=0\ ,$$

and

$$|+,N\rangle\simeq\frac{\Omega_{ei}\sqrt{N+1}}{\Delta}|e,N\rangle+|i,N+1\rangle+\frac{\Omega_{if}\sqrt{N+2}}{\Delta}|f,N+2\rangle\ ,$$
$$|-,N\rangle\simeq\frac{\Omega_{ei}\sqrt{N+1}}{\sqrt{\Delta\Omega(N)}}|e,N\rangle+\frac{\Omega_{if}\sqrt{N+2}}{\sqrt{\Delta\Omega(N)}}|f,N+2\rangle\ , \quad (28)$$
$$|0,N\rangle=\frac{\Omega_{if}\sqrt{N+2}}{\sqrt{\Delta\Omega(N)}}|e,N\rangle-\frac{\Omega_{ei}\sqrt{N+1}}{\sqrt{\Delta\Omega(N)}}|f,N+2\rangle\ .$$

The dressed energies in the Nth manifold are represented in Fig. 5(b). The $|0,N\rangle$ level is unshifted with respect to the $|e,N\rangle, |f,N+2\rangle$ doublet whereas the $|+,N\rangle$ and $|-,N\rangle$ states are shifted by $\hbar\Delta$ and $-\hbar\Omega(N)$, respectively.

Let us now assume that the system is initially in the $|e,N\rangle$ uncoupled state representing the atom in level $|e\rangle$ suddenly introduced in the cavity containing N photons. This state is—to the approximation mentioned above—a linear combination of the two $|-,N\rangle$ and $|0,N\rangle$ dressed eigenstates, separated from each other by $\hbar\Omega$,

$$|e,N\rangle=\frac{\Omega_{ei}\sqrt{N+1}}{\sqrt{\Delta\Omega(N)}}|-,N\rangle+\frac{\Omega_{if}\sqrt{N+2}}{\sqrt{\Delta\Omega(N)}}|0,N\rangle\ . \quad (29)$$

The state of the system at a subsequent time t is simply

$$|e,N(t)\rangle=\frac{\Omega_{ei}\sqrt{N+1}}{\sqrt{\Delta\Omega(N)}}e^{i\Omega(N)t}|-,N\rangle+\frac{\Omega_{if}\sqrt{N+2}}{\sqrt{\Delta\Omega(N)}}|0,N\rangle \tag{30}$$

and the probability of finding at time t the atom in the initial level $|e\rangle$ is

$$P_e^N(t)=|\langle e,N|e,N(t)\rangle|^2 =1-\frac{2\Omega_{ei}^2\Omega_{if}^2(N+1)(N+2)}{\Delta^2\Omega^2(N)}\{1-\cos[\Omega(N)t]\} . \tag{31}$$

In the dressed-atom picture, the system evolution does reduce to a two-level problem in the subspace spanned by the two $|-,N\rangle$ and $|0,N\rangle$ dressed states, provided we assume $|\Omega/\Delta|\ll 1$. Carrying out the exact calculation based on Eqs. (23) and (24) is more cumbersome but not difficult. It merely adds to the main nutation component at frequency $\Omega(N)$ a small contribution oscillating at the much higher frequency Δ, corresponding to the tiny projection of $|e,N\rangle$ on the $|+,N\rangle$ state. This contribution is completely negligible in the maser problem.

Let us now analyze in more detail formula (31). The atom + field system evolves at the two-photon Rabi pulsation $\Omega(N)$ given by Eq. (25), which we can also write as

$$\Omega(N)=A+BN \tag{32}$$

with

$$A=\frac{(\Omega_{ei}^2+2\Omega_{if}^2)}{\Delta} , \tag{33a}$$

$$B=\frac{(\Omega_{ei}^2+\Omega_{if}^2)}{\Delta} . \tag{33b}$$

A is the spontaneous two-photon Rabi frequency which describes the rate at which the atom flip-flops from $|e\rangle$ to $|f\rangle$ and back if it is initially prepared in an empty cavity tuned at the two-photon resonance. This two-photon spontaneous Rabi nutation effect cannot, of course, be accounted for semiclassically. BN, on the other hand, is the stimulated two-photon Rabi frequency, proportional to the photon number, which describes the rate of nutation induced by N initially present photons.

For large N's (classical limit), we have

$$\Omega(N)\simeq BN=\frac{\Omega_{ei}^2+\Omega_{if}^2}{\Delta}N . \tag{34}$$

This result reduces to the intuitive expression given by Eq. (8) for $\Omega_{ei}=\Omega_{if}$, but is generally different for $\Omega_{ei}\neq\Omega_{if}$. This difference can be assigned[22,30] to the dynamical Stark shifts of the levels $|e\rangle$ and $|f\rangle$.

The above calculation shows that the $|e,N\rangle$, $|f,N+2\rangle$ degeneracy is lifted by the atom-field coupling by an amount $\hbar\Omega$. It is possible to derive this result in a slightly different way which will allow us to clearly understand the influence of the Stark effect. Instead of considering globally the triplet manifold $|e,N\rangle, |i,N+1\rangle, |f,N+2\rangle$, let us focus on the degenerate doublet $|e,N\rangle, |f,N+2\rangle$ and analyze the second-order perturbation of this doublet by H_{int}. This approach is legitimate as long as $\Omega_{ei}\sqrt{N+1}, \Omega_{if}\sqrt{N+2}\ll\Delta$. The second-order perturbation matrix to diagonalize in this doublet manifold is

$$V_N=\hbar\begin{bmatrix}\dfrac{\Omega_{ei}^2(N+1)}{\Delta} & \dfrac{\Omega_{ei}\Omega_{if}\sqrt{(N+1)(N+2)}}{\Delta}\\ \dfrac{\Omega_{ei}\Omega_{if}\sqrt{(N+1)(N+2)}}{\Delta} & \dfrac{\Omega_{if}^2(N+2)}{\Delta}\end{bmatrix} . \tag{35}$$

The diagonal matrix elements of V_N represent the Stark shifts of levels $|e\rangle$ and $|f\rangle$ due to the field and the off-diagonal elements describe the coupling between these levels responsible for the Rabi oscillation. When the condition

$$\Omega_{ei}\sqrt{N+1}=\Omega_{if}\sqrt{N+2} \tag{36}$$

is fulfilled, the differential shift between the levels $|e\rangle$ and $|f\rangle$ is zero. Substracting an irrelevant constant, we find that the eigenvalues of V_n are then

$$\pm\frac{\Omega_{ei}\Omega_{if}\sqrt{(N+1)(N+2)}}{\Delta}$$

and the corresponding Rabi frequency is, for large N's,

$$\Omega(N)\simeq\frac{2\Omega_{ei}\Omega_{if}N}{\Delta}$$

in full agreement with Eq. (8).

In general, however, Eq. (36) is not exactly satisfied and we have to take the diagonal part of V_N into account. The eigenvalues of V_N are then

$$E_0=0$$

and

$$E_-=-\hbar\frac{(\Omega_{ei})^2(N+1)+\Omega_{if}^2(N+2)}{\Delta}$$

in agreement with Eqs. (25) and (27).

The difference between expressions (8) and (25) is thus clearly due to the Stark shifts which slightly detune the dressed-state transition from the cavity frequency and thus change the Rabi pulsation. These shifts also modify the maximum transition probability between levels $|e\rangle$

and $|f\rangle$ as is shown by Eq. (31). When Eq. (36) is satisfied, i.e., when the two levels are equally shifted, the atom and the field stay in exact resonance and Eq. (31) reduces to Eq. (7). The Rabi oscillation is then complete [$P_e(t)$ oscillates between 0 and 1]. As soon as Eq. (36) is not fulfilled, the contrast of the Rabi oscillation becomes somewhat smaller than one [the minimum $P_e^N(t)$ value is larger than zero]. The Stark-shift detuning decreases the efficiency of the two-photon transition process between the levels.

In the case of the Rydberg transition we are considering here, Ω_{ei} and Ω_{if} are very close to each other ($\Omega_{ei}/\Omega_{if}\sim 0.97$), and for N much larger than one, Eq. (36) is approximately satisfied so that the Rabi nutation occurs with a contrast close to unity.

We have so far only considered the Rabi oscillation produced by a pure Fock state $|N\rangle$. It is straightforward to generalize Eq. (31) in order to describe the two-photon Rabi nutation in a field having a photon probability distribution $\pi(N)$.[30] When $\Omega(N)/\Delta \ll 1$, we simply get

$$P_e(t)=1-2\sum_N \pi(N)\frac{\Omega_{ei}^2\Omega_{if}^2(N+1)(N+2)}{\Delta^2\Omega^2(N)} \times\{1-\cos[\Omega(N)t]\} \ . \tag{37}$$

$P_e(t)$ merely appears as a sum of elementary Rabi nutation signals weighted by the probability distribution $\pi(N)$. Generalization to the case when $\Omega(N)/\Delta$ is not negligible is straightforward. $P_e(t)$ then includes a small component at frequency Δ. Equation (37) generalizes to the two-photon case similar expressions already derived in the case of ordinary one-photon Rabi oscillation.[32–34] $P_e(t)$ is in this case a superposition of terms oscillating at frequencies proportional to $\sqrt{N}$. The study of this superposition reveals that the Rabi oscillation collapses after some time and then revives after a longer time, the effect being due to the dispersion of elementary frequencies over an infinite but discrete set of values. Considerable theoretical interest has been given to this effect[32,34] which can now be observed with Rydberg-atom—cavity systems.[35] The two-photon version of this effect reveals interesting new features,[30] basically related to the fact that the elementary Rabi frequency is now proportional to N instead of $\sqrt{N}$.

IV. QUANTUM-MECHANICAL THEORY OF THE TWO-PHOTON RYDBERG MASER

We now come back to the study of the field evolution in the two-photon Rydberg maser. The system is still symbolized by Fig. 3; initially excited atoms cross the cavity at a rate t_{at}^{-1}, each atom spending a time t_{int} in the cavity mode.

In a first stage, we assume for simplicity that t_{at} and t_{int} are fixed times. Later on, we will make the analysis more realistic by allowing these times to fluctuate from one atom to the next (random density and velocities in the Rydberg-atom beam).

The condition

$$t_{int} < t_{at} \tag{38}$$

will, however, be always assumed, which means that there is at most one atom interacting at any time with the field. This condition is fulfilled—as seen in Sec. II—in a very-high-Q cavity. It will allow us to keep the theory simple by neglecting all atom-atom correlations in the cavity.

We also separate in this simple approach the atom-field interaction from the field-relaxation process. We will consider that the field is not damped at all during the time each atom crosses the cavity and relaxes only during the time interval $t_{at}-t_{int}$ between the exit of one atom and the entry of the next one. By this separation, we keep as shown below a very simple description of the atom evolution in the cavity and considerably simplify the theory. In order to take realistically into account the actual field relaxation, we must, of course, correspondingly increase the field-relaxation rate so that the damping occurring during $t_{at}-t_{int}$ is on the average the same as if it occurred during the whole time t_{at}. We thus replace in the equation the real cavity-damping time $t_{cav}=Q/\omega$ by an effective time:

$$t'_{cav}=\frac{Q}{\omega}\left[1-\frac{t_{int}}{t_{at}}\right] . \tag{39}$$

This procedure corresponds only, of course, to an approximation becoming increasingly better as t_{int}/t_{at} approaches zero.

We also consider that the atom-field coupling remains constant during t_{int}. Taking into account the true atom-field coupling variation amounts to replacing in the calculation Ωt_{int} by the integral of the Rabi angle over the atom path in the cavity mode. It merely amounts to renormalizing what we call t_{int} in this theory. At last, we neglect the residual blackbody field in the low-temperature cavity; we assume that the field relaxes towards the vacuum state. All the above simplifications are similar to the ones already made in the theory of the one-photon micromaser.[19]

The elementary step in our calculation will consist in computing the change undergone by the field during a cycle of duration t_{at}, between the entry of two consecutive atoms in the cavity. Let us first assume that the cavity contains exactly N photons at the beginning of this cycle. According to the above assumptions, the atom-field evolution during the time t_{int} is given by the Rabi-nutation process analyzed in Sec. III. At time t_{int} the system is thus in a linear superposition of states $|e,N\rangle$ and $|f,N+2\rangle$. The state of the field, obtained by tracing over atomic variables, is thus described by a density operator with a probability

$$\pi(N)=P_e^N(t_{int}) \tag{40}$$

of being in state $|N\rangle$ and

$$\pi(N+2)=1-P_e^N(t_{int}) \tag{41}$$

of being in state $|N+2\rangle$, where P_e^N is given by Eq. (31). This analysis immediately generalizes to a field being initially (time t) in an incoherent superposition of Fock states described by a diagonal density operator, the probability of having N photons in the field being $\pi(N,t)$. At time $t+t_{int}$, we merely have

$$\pi(N,t+t_{\text{int}})=\pi(N,t)P_e^N(t_{\text{int}})$$
$$+\pi(N-2,t)[1-P_e^{N-2}(t_{\text{int}})] \; . \quad (42)$$

Let us emphasize that this simple equation holds only because the field is not damped in the cavity during this time interval, so that the atom-field system is supposed to undergo a pure coherent Rabi precession.

From time $t+t_{\text{int}}$ to time $t+t_{\text{at}}$, $\pi(N,t)$ evolves according to field relaxation alone. $\pi(N,t+t_{\text{at}})$ can be obtained from $\pi(N,t+t_{\text{int}})$ by integrating over the time interval $t_{\text{at}}-t_{\text{int}}$ the well-known field damping equations,[36]

$$\frac{d}{dt}\pi(N,t)=-\frac{N}{t'_{\text{cav}}}\pi(N,t)+\frac{N+1}{t'_{\text{cav}}}\pi(N+1,t) \; . \quad (43)$$

Explicit integration of this differential equation is necessary since the field, at maser threshold, loses about two photons during such a cycle. A first-order approximation of this equation is not precise enough.

By a numerical iteration of transformations (42) and (43), one straightforwardly gets the probability $\pi(N,N_{\text{at}})$ of having N photons in the field after N_{at} atoms have crossed the cavity. This result depends, of course, of the initial condition, i.e., on $\pi(N,0)$. which describes the "triggering" field present in the cavity before the first atom has crossed it. Notice that we have replaced here the time t by N_{at} in the expression of the π's according to the obvious relationship

$$N_{\text{at}}=\frac{t}{t_{\text{at}}} \; . \quad (44)$$

After having computed $\pi(N,N_{\text{at}})$, we get the mean number of photons in the cavity

$$\overline{N}(N_{\text{at}})=\sum_N N\pi(N,N_{\text{at}}) \quad (45)$$

and the field variance

$$V(N_{\text{at}})=\left[\frac{\Delta N^2(N_{\text{at}})}{\overline{N}(N_{\text{at}})}\right]^{1/2}$$
$$=\left[\sum_N \frac{(N^2-\overline{N}^2)\pi(N,N_{\text{at}})}{\overline{N}(N_{\text{at}})}\right]^{1/2} \; . \quad (46)$$

Figures 6(a) and 6(b) present $\overline{N}(N_{\text{at}})$ and $V(N_{\text{at}})$ for $t_{\text{int}}=1.4\times10^{-2}t_{\text{cav}}$, $t_{\text{at}}=3\times10^{-2}t_{\text{cav}}$, and $\Omega_{ei}=\Omega_{if}$. Moreover, Ω_{ei}, Ω_{if}, and Δ are chosen so that $\Omega(N)t_{\text{int}}=\pi$ for $N=40$. All these parameters are realistic values for a two-photon Rydberg maser and close to the values assumed in the qualitative discussion of Sec. II. For the initial field, we have chosen a Poisson distribution with a mean value $\overline{N}=40$,

$$\pi(N,0)=\frac{40^N}{N!}e^{-40} \; . \quad (47)$$

We see on Fig. 6(a) that the field increases in the cavity and reaches—after about 50 cycles—a steady-state value corresponding to $\overline{N}=52$. Figure 6(b) shows the corresponding variance. It decreases from 1 to about 0.55 which means that the maser field is—in these conditions—sub-Poissonian and nonclassical.

The necessity of triggering the two-photon maser appears clearly when comparing Fig. 6(a) with Fig. 7 which represents the variation of $\overline{N}(N_{\text{at}})$ for a maser operating under exactly the same conditions as above, but without any triggering,

$$\pi(N,0)=0 \; . \quad (48)$$

The mean photon number increases only very slightly above zero in this case and reaches a limit of the order of 0.3. This residual field originates in the spontaneous emission of the two-photon transition. This case obviously corresponds to the $\overline{N}=0$ stable solution of the classical discussion of Sec. II, slightly modified to account for spontaneous effects.

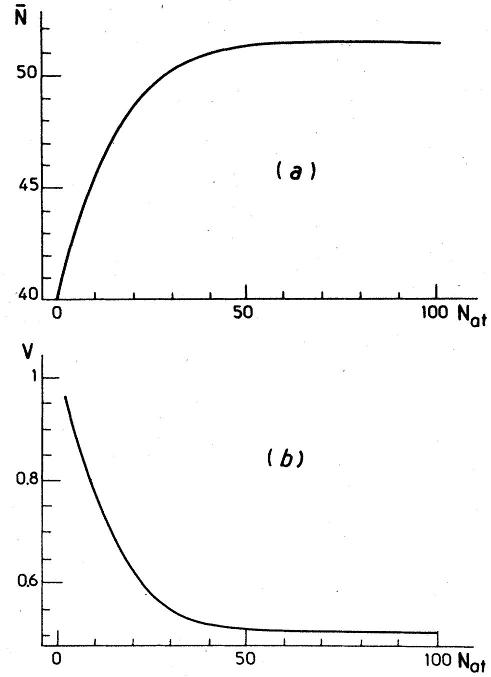

FIG. 6. Evolution of the micromaser as a function of the number N_{at} of atoms having crossed the cavity. (a) average number of stored photons $\overline{N}(N_{\text{at}})$. (b) Photon-number variance $\overline{V}(N_{\text{at}})$. Initial field is an incoherent Poisson field with $\overline{N}=40$. $t_{\text{int}}=1.4\times10^{-2}t_{\text{cav}}$, $t_{\text{at}}=3\times10^{-2}t_{\text{cav}}$, and $\Omega(40)t_{\text{int}}=\pi$.

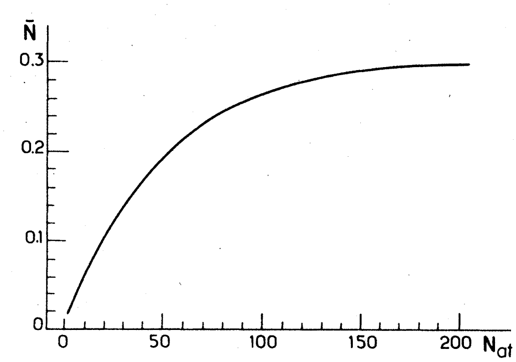

FIG. 7. $\overline{N}(N_{\text{at}})$ for the same conditions as Fig. 6, except that the initial field is in vacuum state.

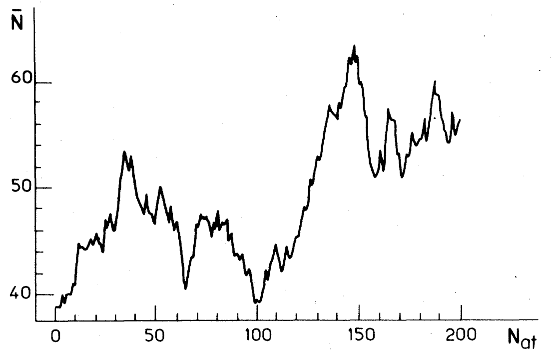

FIG. 8. Average photon number $\overline{N}(N_{at})$ for a two-photon micromaser with fluctuating t_{int} and $t_{at}-t_{int}$. Average values of t_{int} and t_{at} are the same as in Figs. 6 and 7. Mean-square-root deviations are $\Delta t_{int}=5.6\times10^{-3}t_{cav}$, $\Delta(t_{at}-t_{int})=1.1\times10^{-2}t_{cav}$. Triggering field is the same as for Fig. 6.

It is easy to generalize the above model to account for fluctuations of t_{int} and $t_{at}-t_{int}$. We can randomly choose these parameters in each cycle of the calculation, assuming a Maxwellian distribution for $1/t_{int}$ and a Gaussian statistics for $t_{at}-t_{int}$. Figure 8 shows $\overline{N}(N_{at})$ for a system in which t_{int} and t_{at} have the same average values as above (Fig. 6) with a mean-square deviation $\Delta t_{int}=5.6\times10^{-3}t_{cav}$ and $\Delta(t_{at}-t_{int})=1.1\times10^{-2}t_{cav}$. We see that a given realization of the maser field presents now large temporal fluctuations but that, on average, the photon number increases to a value close to the one reached by a fluctuationless system.

The two-photon maser just described corresponds to a system initiated by a statistical mixture of Fock states, i.e., by a triggering field with no priviledged phase. In a practical device the field emission will be most conveniently initiated by a classical coherent field in a Glauber state filling the cavity at time $t=0$. Such a field presents coherences between Fock states with different N's and the $\pi(N)$ probabilities are not enough to fully characterize the field. During the system evolution, all the matrix elements of the field density operator will be coupled together. The above analysis thus corresponds to an approximation in which the effect of the coupling between the diagonal and off-diagonal elements are neglected. Such an approximation needs not be made. One can write exact quantum-mechanical rate equations for the density operator ρ of the combined atom + field system. This operator has matrix elements such as $\rho_{eN,eN'}$, $\rho_{eN,fN'}$, $\rho_{fN,fN'}$ describing atom-field coherences. Numerical solution of these equations followed by tracing over atom variables makes it possible to compute at the end of each cycle the field density operator knowing it at the beginning of the cycle. When this complete approach is taken, there is no need to separate the atom-field interaction from field damping. The only assumption which is kept is that there is one atom at a time in the cavity so that—during each cycle—the atomic medium is a simple two-level system. Solving these more general equations is still feasible if the number of photons is not too large (i.e., around maser threshold). The preliminary results obtained are very close to the above simple calculations for the maser intensity and the photon-number variance.

The main interest of this complete calculation is to yield in addition other interesting quantities such as the maser phase diffusion and the squeezing factor of its field.[8,9] Results of these calculations will be presented elsewhere.

V. CONCLUSION

Two features of the Rydberg two-photon micromaser described above are very promising in order to eliminate other competing processes which could prevent the oscillator from working as expected: (i) The oscillation is sustained by a closed cavity in its fundamental mode, (ii) the triggering field and the steady-state field in the cavity are exceedingly small.

These properties make it very unlikely that another nonlinear process could build up and deplete the initial population inversion. The most likely candidate would be the one-photon amplification on the $nS\to(n-1)P_{3/2}$ transition towards the intermediate level $|\,i\,\rangle$. This transition is detuned by $\Delta/2\pi$ from the triggering field frequency ω. This detuning is 40 000 times larger than the cavity width $\omega/Q\sim1$ kHz for the $40S\to39S$ transition in Rb. On the other hand, the broadening of the one-photon line due to saturation is in frequency units $(1/2\pi)(\Omega_{ei}\sqrt{N})$, i.e., 10^5 Hz, about 50 times smaller than the detuning $\Delta/2\pi$. No significant amplification can occur at frequency $\omega+\Delta$ under these conditions.

Note, however, that the competition with one-photon emission is much more damaging if one chooses the smaller detuning corresponding to the $39S\to38P\to38S$ cascade. $\Delta/2\pi$ is only ~0.5 MHz in this case, of the order of $\Omega_{ei}/2\pi$. This transition does not seem for this reason to be a good candidate for the two-photon maser.

In conclusion, the feasibility of a two-photon maser oscillator operating on the $40S\to39S$ transition in Rb (or $44S\to43S$ transition in cesium) is established. Experimental investigations in Rb are in progress in our laboratory using Nb superconducting cavities at 2 K.

[1]P. P. Sorokin and N. Braslau, IBM J. Res. Develop. **8**, 177 (1964).
[2]A. M. Prokhorov, Science **149**, 828 (1965).
[3]V. S. Letokhov, Pis'ma Zh. Eksp. Teor. Fiz. **7**, 284 (1968) [JETP Lett. **7**, 221 (1968)].
[4]L. R. Estes, L. M. Narducci, and B. Shammas, Lett. Nuovo Cimento **1**, 775 (1971).
[5]L. M. Narducci, W. W. Eidson, P. Furcinitti, and D. C. Eteson, Phys. Rev. A **16**, 1665 (1977).
[6]R. L. Carman, Phys. Rev. A **12**, 2048 (1975).
[7]H. P. Yuen, Appl. Phys. Lett. **26**, 505 (1975).
[8]H. P. Yuen, Phys. Lett. **51 A**, 1 (1975).

[9]H. P. Yuen, Phys. Rev. A **13**, 226 (1976).
[10]T. Hoshimiya, A. Yamagishi, N. Tanno, and H. Inaba, Jpn. J. Appl. Phys. **17**, 2177 (1978).
[11]N. Nayak and B. K. Mohanty, Phys. Rev. A **19**, 1204 (1979).
[12]B. Nikolaus, D. Z. Zhang, and P. E. Toschek, Phys. Rev. Lett. **47**, 171 (1981).
[13]L. Moi, P. Goy, M. Gross, J. M. Raimond, C. Fabre and S. Haroche, Phys. Rev. A **27**, 2043 (1983); P. Goy, L. Moi, M. Gross, J. M. Raimond, C. Fabre, and S. Haroche, Phys. Rev. A **27**, 2065 (1983).
[14]P. Goy, J. M. Raimond, M. Gross, and S. Haroche, Phys. Rev. Lett. **50**, 1903 (1983).
[15]D. Meschede, H. Walther, and G. Müller, Phys. Rev. Lett. **54**, 551 (1985).
[16]S. Haroche, *New Trends in Atomic Physics,* edited by G. Grynberg and R. Stora (North-Holland, Amsterdam, 1984).
[17]S. Haroche and J. M. Raimond, in *Advances in Atomic and Molecular Physics,* edited by D. R. Bates and R. Bederson (Academic, London, 1985), Vol. 20.
[18]J. A. C. Gallas, G. Leuchs, H. Walther, and H. Figger, in *Advances in Atomic and Molecular Physics,* edited by D. R. Bates and R. Bederson (Academic, London, 1985), Vol. 20.
[19]P. Filipowicz, J. Javanainen, and P. Meystre, Phys. Rev. A **34**, 3077 (1986).
[20]D. Grischkowsky, M. M. T. Loy, and P. F. Liao, Phys. Rev. A **12**, 2514 (1975).
[21]R. G. Brewer and E. L. Hahn, Phys. Rev. A **11**, 1641 (1975).
[22]M. Takatsuji, Phys. Rev. A **11**, 619 (1975).
[23]Of course, the $S_{1/2}$ and $P_{3/2}$ levels are in fact degenerate. However, only one substate in each of these levels is concerned in this problem: we call $|e\rangle$ the level $|nS,m_S=\pm\frac{1}{2}\rangle$ in which the atom is initially prepared. If the quantization axis is chosen along the linear polarization direction of the cavity field, only the sublevels $|i\rangle=|n-1P_{3/2},m=m_S\rangle$ and $|f\rangle=|n-1S_{1/2},m=m_S\rangle$ are concerned. We neglect here the hyperfine structure of the nS and nP states which is hardly resolved in a realistic experiment.
[24]P. Goy, J. M. Raimond, G. Vitrant, C. Fabre, S. Haroche, and M. Gross, *Precision Measurements and Fundamental Constants II,* Natl. Bur. Stand. (U.S.) Spec. Publ. No. 617, edited by B. N. Taylor and W. D. Phillips (U.S. GPO, Washington, D.C., 1982); C. Fabre, S. Haroche, and P. Goy, Phys. Rev. A **22**, 778 (1980).
[25]P. Goy, J. M. Raimond, G. Vitrant, and S. Haroche, Phys. Rev. A **26**, 2733 (1982).
[26]D. Meschede, Dissertation, Fakulät für Physik der Ludwig-Maximilians Universität München, 1984.
[27]P. Goy, J. Liang, M. Gross, and S. Haroche, Phys. Rev. A **34**, 2889 (1986).
[28]G. Müller, Dissertation, Universität gesamthochschule Wuppertal, Wuppertal, 1983.
[29]P. Fillipowicz, P. Meystre, G. Rempe, and H. Walther, Opt. Acta **32**, 1105 (1985).
[30]H. I. Yoo and J. H. Eberly, Phys. Rep. **118**, 239 (1985).
[31]S. Haroche, Ann. Phys. (Paris) **6**, 189 (1971); C. Cohen-Tannoudji and S. Reynaud, J. Phys. B **10**, 345 (1977).
[32]A. Faist, E. Geneux, P. Meystre, and A. Quattropani, Helv. Phys. Acta. **45**, 956 (1972).
[33]J. H. Eberly, N. B. Narozhny, and J. J. Sanchez-Mondragon, Phys. Rev. Lett. **44**, 1323 (1980).
[34]P. L. Knight and P. M. Radmore, Phys. Rev. A **26**, 676 (1982).
[35]G. Rempe and H. Walther, in *Methods of Laser Spectroscopy,* edited by Y. Prior, A. Ben-Reuven, and M. Rosenblum (Plenum, New York, 1986), p. 11.
[36]G. S. Agarwal, in *Quantum Statistical Theories of Spontaneous Emission and their Relation to other Approaches,* Vol. 70 of *Springer Tracts in Modern Physics,* edited by G. Hohler (Springer-Verlag, Berlin, 1974); W. H. Louisell, *Quantum Statistical Properties of Radiation* (Wiley, New York, 1973).